



Explosive Synchronization in Adaptive and Multilayer Networks

Xiyun Zhang,¹ Stefano Boccaletti,^{2,3,*} Shuguang Guan,¹ and Zonghua Liu^{1,†}

¹Department of Physics, East China Normal University, Shanghai 200062, China

²CNR—Institute of Complex Systems, Via Madonna del Piano 10, 50019 Sesto Fiorentino, Florence, Italy

³The Italian Embassy in Israel, 25 Hamered Street, 68125 Tel Aviv, Israel

(Received 6 October 2014; published 21 January 2015)

At this time, explosive synchronization (ES) of networked oscillators is thought of as being rooted in the setting of specific microscopic correlation features between the natural frequencies of the oscillators and their effective coupling strengths. We show that ES is, in fact, far more general and can occur in adaptive and multilayer networks in the absence of such correlation properties. We first report evidence of ES for single-layer networks where a fraction f of the nodes have links adaptively controlled by a local order parameter, and we then extend the study to a variety of two-layer networks with a fraction f of their nodes coupled with each other by means of dependency links. In the latter case, we give evidence of ES regardless of the differences in the frequency distribution, in the topology of connections between the layers, or both. Finally, we provide a rigorous, analytical treatment to properly ground all of the observed scenarios and to advance the understanding of the actual mechanisms at the basis of ES in real-world systems.

DOI: 10.1103/PhysRevLett.114.038701

PACS numbers: 89.75.Hc, 05.45.Xt, 89.75.-k

Recently, it was pointed out that the transition of an ensemble of networked phase oscillators from incoherence to synchronization can be first order like, discontinuous and irreversible, called explosive synchronization (ES). This discovery is of huge significance, as examples of abrupt transitions in real-world networks [1] include epileptic seizures in the brain [2], the cascading failure of power grids [3], and the jamming of the Internet [4]. Since its discovery in 2005 [5], ES has been paid great attention [6–14]. The accepted state of knowledge on this matter is, hence, that ES has a basic microscopic root in the setting of local correlation features (either imposed *ad hoc* [6,7] or spontaneously emerging [8–14]) between the natural frequency of a networked oscillator and its degree, or effective coupling strength. In this Letter, we fundamentally revisit the issue and answer the following question: Is it possible to observe ES *without* the presence of *any kind* of correlation features? We first consider a network where a fraction f of the nodes is adaptively controlled by a local order parameter, and we show that ES emerges, indeed, when the value of f is over a critical value f_c . We then extend the study to multilayer networks. Precisely, we show that ES is a generic feature of two-layered networks, when a fraction f of their nodes are coupled with each other by means of *dependency* links. Further, we present a rigorous theoretical analysis of the mean field, which accounts for all of the described scenarios and allows us to we formulate a main conclusion: All previous studies on ES can, in fact, be unified into a common root, that of suppressing the formation of giant clusters.

We begin by considering a network of N Kuramoto-like phase oscillators, with an explicit fraction f of the nodes adaptively controlled by a local order parameter [15]. The evolution of each oscillator is ruled by

$$\dot{\theta}_i = \omega_i + \lambda \alpha_i \sum_{j=1}^N A_{ij} \sin(\theta_j - \theta_i), \quad (1)$$

where $i = 1, \dots, N$, ω_i (θ_i) is the natural frequency (the instantaneous phase) of the i th oscillator, λ is the overall coupling strength, $k_i = \sum_{j=1}^N A_{ij}$ is the degree of node i , and A_{ij} are the elements of the network's adjacency matrix ($A_{ij} = 1$ when the nodes i and j are connected, and $A_{ij} = 0$ otherwise). As compared to previous studies, the key feature of Eq. (1) is the presence of the parameter α_i . To define α_i , we refer to the instantaneous local order parameter for the i th oscillator, defined as $r_i(t)e^{i\phi} = (1/k_i) \sum_{j=1}^{k_i} e^{i\theta_j}$. By definition, $0 \leq r_i \leq 1$, and ϕ denotes the phase averaged over the ensemble of neighbors. Then, we randomly choose a fraction f of the network's nodes and set, for all of them, $\alpha_i = r_i$. For the remaining fraction $1 - f$ of nodes, $\alpha_i = 1$.

The degree of phase coherence in the network can be measured by means of the global order parameter R defined by $Re^{i\Psi} = (1/N) \sum_{j=1}^N e^{i\theta_j}$, where $0 \leq R \leq 1$ and Ψ denote the average network's phase. In our first numerical simulations, we draw the set of frequencies $\{\omega_i\}$ in Eq. (1) from a random homogeneous distribution $g(\omega)$ in the range $[-1, 1]$, and we consider an Erdős-Rényi (ER) network with size $N = 1000$ and average degree $\langle k \rangle = (1/N) \sum_{i=1}^N k_i = 12$. We increase (decrease) the coupling strength λ adiabatically with an increment (decrement) $\delta\lambda = 0.01$ from $\lambda = 0$ ($\lambda = 0.5$) and compute the stationary value of R for each λ [16] during the forward (backward) transition from the incoherent to the phase synchronized state. Figure 1 reports R vs λ for $f = 1$. The presence of an abrupt transition with an associated hysteric loop in R is evident, indicating the occurrence of ES,

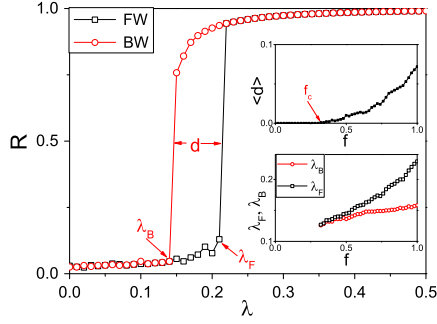


FIG. 1 (color online). Forward (black line with squares) and backward (red line with circles) synchronization transitions for a single network with $N = 1000$ and $f = 1$. The upper and lower insets report the dependence of the average $\langle d \rangle$ and the transition points λ_F and λ_B , respectively, on f for ten realizations. See the text for specifications on the network topology and on the frequency distribution.

as shown in Eq. (1). Denoting by d the width of such a hysteric loop, we calculate the value of d for different realizations of a randomly chosen fraction f of nodes and then obtain the ensemble average $\langle d \rangle$. The upper inset of Fig. 1 reports the dependence of $\langle d \rangle$ on f and shows the existence of a critical value f_c where $\langle d \rangle$ passes from being zero (i.e., a second-order phase transition) to a finite value. For each $f > f_c$, there is a pair of corresponding forward and backward transition points λ_F and λ_B , with $d = \lambda_F - \lambda_B$. It is mandatory here to remark that what is reported here is based explicitly on numerical results, which, by their intrinsic nature, are (evidently) the fruit of a finite size investigation. Further insights on the critical value f_c will instead be reported by us elsewhere. The lower inset of Fig. 1 reports the dependence of λ_F and λ_B on f .

Our second step is showing the generality and scalability of the scenario for the case of multilayer networks [17], with different topological and frequency configurations. For this purpose, we construct two independent networks (I and II) with the same size N . Again, we randomly choose a fraction f of the nodes from each of the two layers and let them be one to one coupled with each other by forming dependency links [18]. For convenience, we let the coupled pairs of nodes have the same index i and we also let the uncoupled nodes on the two layers have a one-to-one correspondence with the same index i . The equations of motion can be written as

$$\begin{aligned}\dot{\theta}_{i,1} &= \omega_{i,1} + \lambda \alpha_{i,1} \sum_{j=1}^{k_{i,1}} \sin(\theta_{j,1} - \theta_{i,1}), \\ \dot{\theta}_{i,2} &= \omega_{i,2} + \lambda \alpha_{i,2} \sum_{j=1}^{k_{i,2}} \sin(\theta_{j,2} - \theta_{i,2}),\end{aligned}\quad (2)$$

where $i = 1, \dots, N$ and the subscripts 1,2 stand for the layers I and II, respectively. In Eq. (2), the average degree

is $\langle k_1 \rangle = (1/N) \sum_{i=1}^N k_{i,1}$ ($\langle k_2 \rangle = (1/N) \sum_{i=1}^N k_{i,2}$) for layer I (II), and the parameters $\alpha_{i,1}$ and $\alpha_{i,2}$ account for the coupling between the two layers. Precisely, we set $\alpha_{i,1} = r_{i,2}$ and $\alpha_{i,2} = r_{i,1}$ if the pair of nodes i is part of the fraction f of coupled nodes (otherwise, we set $\alpha_{i,1} = \alpha_{i,2} = 1$), where $r_{i,1}$ and $r_{i,2}$ are defined by $r_{i,1} e^{i\phi_1} = (1/k_{i,1}) \sum_{j=1}^{k_{i,1}} e^{i\theta_{j,1}}$ and $r_{i,2} e^{i\phi_2} = (1/k_{i,2}) \sum_{j=1}^{k_{i,2}} e^{i\theta_{j,2}}$. In other words, a group of oscillators in layer I is here adaptively controlled by the local order parameters of the corresponding nodes on layer II, and vice versa.

Let R_1 and R_2 be the global order parameters of layers I and II, respectively, defined by $R_1 e^{i\Psi_1} = (1/N) \sum_{j=1}^N e^{i\theta_{j,1}}$ and $R_2 e^{i\Psi_2} = (1/N) \sum_{j=1}^N e^{i\theta_{j,2}}$. In our simulations, layer I is fixed as a random ER network with average degree $\langle k_1 \rangle = 12$, and we draw the set frequencies $\{\omega_{i,1}\}$ from a random homogeneous distribution in the range $[-1, 1]$. Instead, in the following, we will vary both the topology and the frequency distribution $g(\omega_{i,2})$ characterizing layer II. First, we let it be an independent random ER network with the same average degree $\langle k_2 \rangle = 12$, and we let its frequencies $\{\omega_{i,2}\}$ be drawn from an independent random homogeneous distribution in the range $[-1, 1]$. Figure 2(a) shows the dependence of R_1 and R_2 on λ for the case of $f = 1$. One clearly sees that ES occurs simultaneously in both layers. To figure out the dependence of $\langle d \rangle$ on f , we make different realizations where the coupled networks

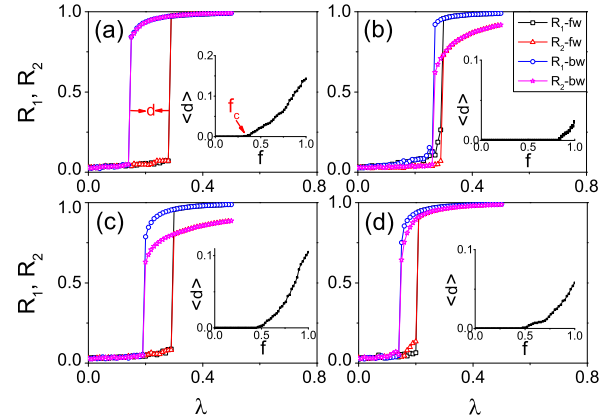


FIG. 2 (color online). Synchronization transitions in two-layer networks for $N = 1000$ and $f = 1$. In all plots, squares and circles (triangles and stars) are used for denoting the forward and backward transition of R_1 (R_2), and the insets show the corresponding dependence of $\langle d \rangle$ on f for ten realizations. Layer I is fixed as a random ER network with average degree $\langle k_1 \rangle = 12$ and having a random homogeneous distribution of frequencies in the range $[-1, 1]$. Layer II has different specifications, as follows: (a) it is another ER network with $\langle k_2 \rangle = 12$, and $g(\omega_{i,2})$ is an independent homogeneous distribution in the range $[-1, 1]$; (b) it is an ER network with $\langle k_2 \rangle = 6$ and $g(\omega_{i,2})$ is the same as in (a); (c) the same as in (a), but $g(\omega_{i,2})$ is now a Lorentzian distribution (see the text for a definition) with $\omega_0 = 0$ and $\gamma = 0.5$; (d) a BA network with $\langle k_2 \rangle = 12$ and $g(\omega_{i,2})$ being the same as in (a).

are reproduced with different initial conditions, and the fraction f at each layer is randomly chosen. Once again, the inset of Fig. 2(a) shows the dependence of $\langle d \rangle$ on f , which, analogously with Fig. 1, indicates the presence of a *numerically evaluated* critical value f_c for the setting of the irreversible, hysteretic transition. Second, we let the average degree $\langle k_2 \rangle$ of layer II change from 12 to 6, while keeping all of the other parameters unchanged. The results for $f = 1$ are now shown in Fig. 2(b), with the inset again reporting the dependence of $\langle d \rangle$ on f . Once again ES sets in, though the associated values of d and f_c are, respectively, smaller and larger. As a third step, we now let the frequency distribution $g(\omega_{i,2})$ change from a homogeneous to a Lorentzian distribution $g(\omega) = (1/\pi)[\gamma/(\omega - \omega_0)^2 + \gamma^2]$ with central frequency $\omega_0 = 0$ and γ (the half width at half maximum [19]) equal to 0.5, while keeping all of the other parameters the same as those of Fig. 2(a). A significant difference between the homogeneous and Lorentzian distributions is that the latter is heterogeneous with an approximate power law on ω . Nonetheless, Fig. 2(c) and its inset clearly indicate the setting of ES. Finally, we change even the topology of layer II from an ER network to a Barabási-Albert (BA) network [20], while keeping all other parameters as in the case of Fig. 2(a). Notice that, in the latter situation, the topologies of the two layers are essentially different. Once again, the results [reported in Fig. 2(d)] are similar to those of Figs. 2(a)–2(c) and demonstrate the existence of both a hysteretic loop and a critical f_c associated with the transition to synchronization.

The Supplemental Material [21] reports full evidence that the scenarios observed in both Fig. 1 and Fig. 2 occur in the *absence* of correlation features between the frequencies of the oscillators and their degrees, or the coupling strength.

With the exception of the dependency of f_c on the parameter λ , it is also interesting to study how f_c numerically depends on the system parameter $\langle k \rangle$. We find that, in the case of a single network, f_c decreases monotonically with the increase of $\langle k \rangle$. As in the case of the duplex with the two layers having an equal size N , we consistently observe a similar decreasing phenomenon, giving a hint that denser connections actually make ES occur easily. Figure 2 in our Supplemental Material [21] actually accounts for the overall, relative scenario.

We now stop for a moment and try to recall (at this stage) the remarkable conclusions that can be drawn from what we have reported so far. ES is a generic property of adaptive networks, as well as multilayer networks, as far as the coupling form used in Eqs. (1) and (2) is taken into account. This has two main implications: (i) it sharply contrasts with previous conclusions that a positive correlation between the natural frequencies of oscillators and their effective couplings is the essential root for ES; and (ii) the passage from a first- to a second-order transition is actually controlled

here by the coupled fraction f of nodes for which adaptation is effective.

The next step of our study, then, is moving to some theoretical analysis, in order to grasp the essential ingredients at the origin of the observed scenarios. To that purpose, we consider the case of Fig. 1, with $f = 1$ as an example. One has

$$\dot{\theta}_i = \omega_i + \lambda r_i^2 k_i \sin(\Psi - \theta_i), \quad (3)$$

where $\dot{\Psi} = \Omega$ is the group angular velocity. In the mean-field framework, $r_i = R$. Letting $\Delta\theta_i = \theta_i - \Psi$, Eq. (3) becomes $\Delta\dot{\theta}_i = \omega_i - \Omega - \lambda R^2 k_i \sin(\Delta\theta_i)$.

If $|\omega_i - \Omega| < \lambda R^2 k_i$, then $\Delta\theta_i$ reaches a fixed point defined by $\sin(\Delta\theta_i) = (\omega_i - \Omega)/\lambda R^2 k_i$, indicating that the oscillator i becomes phase locked to the mean field. Otherwise, $\Delta\theta_i$ never reaches a fixed point, indicating that oscillator i drifts at all times. Considering that the natural frequency distribution $g(\omega_i)$ is symmetric here, we have the average frequency Ω vanishing. Thus, for the phase-locked oscillators, one has

$$\Delta\theta_i = \arcsin\left(\frac{\omega_i}{\lambda R^2 k_i}\right), \quad |\omega_i| \leq \lambda R^2 k_i. \quad (4)$$

Based on Eq. (4), one can calculate the order parameter R . Noticing that R can be redefined as $R = \sum_{j=1}^N k_j r_j / \sum_{j=1}^N k_j$ [22,23], which gives $R e^{i\Psi} = (1/N\langle k \rangle) \sum_{j=1}^N k_j e^{i\theta_j}$, and that the drifting oscillators do not contribute to R [8,24], one has

$$R = \frac{1}{N\langle k \rangle} \sum_{|\omega_j| \leq \lambda R^2 k_j} k_j \cos(\Delta\theta_j). \quad (5)$$

Substituting Eq. (4) into Eq. (5) one eventually obtains $R = (1/N\langle k \rangle) \sum_{|\omega_j| \leq \lambda R^2 k_j} k_j \sqrt{1 - (\omega_j/\lambda R^2 k_j)^2}$. Replacing the summation by an integration, the contribution of the locked oscillators to the order parameter is therefore

$$R = \frac{1}{\langle k \rangle} \int_{|\omega| \leq \lambda R^2 k} h(k, \omega) k \sqrt{1 - \left(\frac{\omega}{\lambda R^2 k}\right)^2} d\omega dk, \quad (6)$$

where $h(k, \omega)$ is the joint distribution and can be written as $h(k, \omega) = P(k)g(\omega)$, with $P(k)$ being the degree distribution of the network.

If repeated for the case of Eq. (2), the same treatment yields

$$\begin{aligned} R_1 &= \frac{1}{\langle k_1 \rangle} \int_{C_1} h(k_1, \omega_1) k_1 \sqrt{1 - \left(\frac{\omega_1}{\lambda R_1 R_2 k_1}\right)^2} d\omega_1 dk_1, \\ R_2 &= \frac{1}{\langle k_2 \rangle} \int_{C_2} h(k_2, \omega_2) k_2 \sqrt{1 - \left(\frac{\omega_2}{\lambda R_1 R_2 k_2}\right)^2} d\omega_2 dk_2, \end{aligned} \quad (7)$$

where $C_{1,2} \equiv |\omega_{1,2}| \leq \lambda R_1 R_2 k_{1,2}$ are the integration domains, $h(k_1, \omega_1) = P(k_1)g(\omega_1)$, and $h(k_2, \omega_2) = P(k_2)g(\omega_2)$, with $P(k_1)$ and $P(k_2)$ being the degree distributions of layers I and II, respectively.

Figure 3 in our Supplemental Material [21] reports the solutions of Eqs. (6) and (7). In both cases [illustrated by Figs. 3(a) and 3(b)], it is easy to notice the presence of an unstable middle branch, which is responsible for the hysteretic loop associated to ES and is observed in Figs. 1 and 2.

Our analytic results allow, actually, for a better and deeper understanding of the intimate causes of ES, and in particular of the microscopic mechanisms that are at the basis of the arousal of explosiveness in the transition. Indeed, if one considers the usual Kuramoto model $\dot{\theta}_i = \omega_i + \lambda \sum_{j=1}^N A_{ij} \sin(\theta_j - \theta_i)$ for the common second-order phase transition and develops the same mean-field treatment, one obtains that the formula for the order parameter is

$$R = \frac{1}{\langle k \rangle} \int_{|\omega| \leq \lambda Rk} h(k, \omega) k \sqrt{1 - \left(\frac{\omega}{\lambda Rk}\right)^2} d\omega dk. \quad (8)$$

Now, a distinctive difference between Eq. (8) and Eq. (6) is that the integration range $|\omega| \leq \lambda Rk$ in Eq. (8) is replaced by $|\omega| \leq \lambda R^2 k$ in Eq. (6), which results in the following, remarkable consequence. For the backward curves in Figs. 1 and 2, one has $R \approx R^2 \approx 1$, and thus the difference between R and R^2 is not that large. Instead, for the forward curves of the transition, one has $R \approx 0$, and thus the difference between R and R^2 is significant there; i.e., R^2 will be much smaller than R . Notice, further, that the integration domains in Eqs. (8) and (6) actually determine the fraction of oscillators belonging to the main synchronization cluster. In other words, larger synchronized clusters are forbidden to be formed in Eq. (6), analogous with the suppressive rule discussed in Ref. [13]. In detail, in the usual case of a second-order transition, the oscillators with closer natural frequencies will first form small synchronized clusters and then these clusters will gradually grow up and merge with the increase of the coupling strength, until eventually forming a giant cluster. On the contrary, in the present case, the factor R^2 in the integration domain has the effect of actually *suppressing* the merging of small synchronized clusters. Thus, with the increase of λ , more and more free oscillators will be attracted to each of the distinct clusters, but these clusters are prevented from merging with each other. Eventually, when no more free oscillators are left, a discontinuous and abrupt behavior of R will show up as a consequence of the sudden collapse of all clusters.

Note that the above discussion holds for the case $f = 1$. When $f < 1$, the oscillators can actually be divided into two groups, the controlled fraction f and the free fraction $1 - f$. The oscillators in the controlled fraction have a

behavior similar to that of the case $f = 1$, while those in the fraction $1 - f$ will behave similarly to Eq. (8). The controlled group f and the free group $1 - f$ are in fact interconnected, and the behavior of the free part $1 - f$ will be influenced by the controlled part f , thus implying that the merging of small clusters in the free part $1 - f$ will again be suppressed. The thermodynamic limit of this interplay will soon be reported elsewhere. For the time being, we emphasize that the idea of coupling on a fraction of elements can be also used in different contexts, such as achieving generalized synchronization in autonomous dynamical systems [25], and for the occurrence of complete or generalized chaos synchronization [26].

The most remarkable conclusion of our study is therefore that ES has, indeed, a microscopic root, but this root is essentially to be found in *no matter what* mechanism is able to suppress the formation of a giant synchronization cluster. While a positive correlation between the oscillators' natural frequencies and their degrees [6,7] or coupling strength [9–11] has the effect of suppressing the formation of *any* synchronization cluster, in the present case (i.e., in the absence of any specific correlation features), the network nodes are initially able to form small *independent* synchronized clusters, each one of them being able to further grow with the increase of the coupling strength, and the suppression mechanism acts instead by impeding the merging process of the clusters. We cannot, therefore, exclude the possibility that even other forms of implementing such a basic suppressive rule, originating possibly from still unrevealed microscopic sources, would equally determine the arousal of ES in networked systems.

In conclusion, we reported on the setting of abrupt and explosive synchronization in adaptive and multilayer networks, where it is observable even without the requirement of correlations between natural frequencies and effective couplings of the networks' nodes. Our results are fully robust against large variations in the network topologies and frequency distributions. Based on these findings and in contrast with the accepted state of knowledge on the subject, we can safely conclude that the necessary condition for ES is the existence of a microscopic suppressive rule able to prevent (in one way or another) the formation of a giant synchronization cluster.

Work was partially supported by the National Natural Science Foundation of China under Grants No. 11135001, No. 11375066, and No. 11075056, and the 973 Program under Grant No. 2013CB834100.

* stefano.boccaletti@gmail.com

† zhliu@phy.ecnu.edu.cn

- [1] S. Boccaletti, V. Latora, Y. Moreno, M. Chavez, and D.-U. Hwang, *Phys. Rep.* **424**, 175 (2006).
- [2] B. M. Adhikari, C. M. Epstein, and M. Dhamala, *Phys. Rev. E* **88**, 030701(R) (2013).

- [3] S. V. Buldyrev, R. Parshani, G. Paul, H. E. Stanley, and S. Havlin, *Nature (London)* **464**, 1025 (2010).
- [4] B. A. Huberman and R. M. Lukose, *Science* **277**, 535 (1997).
- [5] D. Pazó, *Phys. Rev. E* **72**, 046211 (2005).
- [6] J. Gómez-Gardeñes, S. Gómez, A. Arenas, and Y. Moreno, *Phys. Rev. Lett.* **106**, 128701 (2011).
- [7] I. Leyva, R. Sevilla-Escoboza, J. M. Buldú, I. Sendiña-Nadal, J. Gómez-Gardeñes, A. Arenas, Y. Moreno, S. Gómez, R. Jaimes-Reategui, and S. Boccaletti, *Phys. Rev. Lett.* **108**, 168702 (2012).
- [8] T. K. D. M. Peron and F. A. Rodrigues, *Phys. Rev. E* **86**, 056108 (2012); **86**, 016102 (2012); B. C. Coutinho, A. V. Goltsev, S. N. Dorogovtsev, and J. F. F. Mendes, *Phys. Rev. E* **87**, 032106 (2013); W. Liu, Y. Wu, J. Xiao, and M. Zhan, *Europhys. Lett.* **101**, 38002 (2013); P. Ji, T. K. D. M. Peron, P. J. Menck, F. A. Rodrigues, and J. Kurths, *Phys. Rev. Lett.* **110**, 218701 (2013).
- [9] I. Leyva, I. Sendiña-Nadal, J. A. Almendral, A. Navas, S. Olmi, and S. Boccaletti, *Phys. Rev. E* **88**, 042808 (2013).
- [10] X. Zhang, X. Hu, J. Kurths, and Z. Liu, *Phys. Rev. E* **88**, 010802(R) (2013).
- [11] I. Leyva, A. Navas, I. Sendiña-Nadal, J. A. Almendral, J. M. Buldú, M. Zanin, D. Papo, and S. Boccaletti, *Sci. Rep.* **3**, 1281 (2013).
- [12] P. Li, K. Zhang, X. Xu, J. Zhang, and M. Small, *Phys. Rev. E* **87**, 042803 (2013); L. Zhu, L. Tian, and D. Shi, *Phys. Rev. E* **88**, 042921 (2013).
- [13] X. Zhang, Y. Zou, S. Boccaletti, and Z. Liu, *Sci. Rep.* **4**, 5200 (2014).
- [14] G. Su, Z. Ruan, S. Guan, and Z. Liu, *Europhys. Lett.* **103**, 48004 (2013).
- [15] F. Dorfler and F. Bullo, *SIAM J. Control Optim.* **50**, 1616 (2012). This paper shows an example of a power grid where the coupling is controlled by a local variable. It is shown that the power grid can be simplified into a nonuniform Kuramoto model by $D_i \dot{\theta}_i = \omega_i - \sum_{j=1}^N P_{ij} [\cos(\phi_{ij}) \sin(\theta_i - \theta_j) + \sin(\phi_{ij}) \cos(\theta_i - \theta_j)]$, where $\cos \phi_{ij}$ and $\sin \phi_{ij}$ represent the local controller.
- [16] The stationary value of R is calculated as a longtime average (over a time $T_a = 50\,000$ time steps) of the order parameter, after a sufficiently large transient time ($T_t = 200\,000$ time steps) has elapsed.
- [17] S. Boccaletti, G. Bianconi, R. Criado, C. I. del Genio, J. Gómez-Gardeñes, M. Romance, I. Sendiña-Nadal, Z. Wang, and M. Zanin, The structure and dynamics of multilayer networks, *Phys. Rep.* **544**, 1 (2014).
- [18] R. Parshani, S. V. Buldyrev, and S. Havlin, *Proc. Natl. Acad. Sci. U.S.A.* **108**, 1007 (2011).
- [19] P. C. Matthews, R. E. Mirollo, and S. H. Strogatz, *Physica (Amsterdam)* **52D**, 293 (1991).
- [20] R. Albert and A.-L. Barabási, *Rev. Mod. Phys.* **74**, 47 (2002).
- [21] See Supplemental Material at <http://link.aps.org/supplemental/10.1103/PhysRevLett.114.038701> for details about Fig. 1 that shows there is no correlation between the natural frequency and local coupling strength.
- [22] J. G. Restrepo, E. Ott, and B. R. Hunt, *Phys. Rev. E* **71**, 036151 (2005).
- [23] T. Ichinomiya, *Phys. Rev. E* **70**, 026116 (2004).
- [24] P. S. Skardal and A. Arenas, *Phys. Rev. E* **89**, 062811 (2014).
- [25] O. Alvarez-Llamoza and M. G. Cosenza, *Phys. Rev. E* **78**, 046216 (2008).
- [26] G. Paredes, O. Alvarez-Llamoza, and M. G. Cosenza, *Phys. Rev. E* **88**, 042920 (2013).